

Supporting Information

Nanoscale Zero-Valent Iron in Mesoporous Carbon (nZVI@C): Stable Nanoparticles for Metal Extraction and Catalysis

*Wei Teng^{a,†}, Jianwei Fan^{a,†}, Wei Wang^a, Nan Bai^a, Rui Liu^c, Yang Liu^b, Yonghui
Deng^{b, d}, Biao Kong^b, Jianping Yang^a, Dongyuan Zhao^{b*} and Wei-xian Zhang^{a*}*

^a State Key Laboratory for Pollution Control, School of Environmental Science and Engineering, Tongji University, Shanghai, China 200092

^b Department of Chemistry, Laboratory of Advanced Materials, State Key Laboratory of Molecular Engineering of Polymers, Shanghai Key Laboratory of Molecular Catalysis and Innovative Materials, Collaborative Innovation Center of Chemistry for Energy Materials (iChEM), Fudan University, Shanghai 200433, P. R. China.

^c Key Laboratory of Advanced Civil Engineering Material, Ministry of Education, School of Materials Science and Engineering, and Institute for Advanced Study, Tongji University, Shanghai, China 201804

^d State Key Lab of Transducer Technology, Shanghai Institute of Microsystem and Information Technology, Chinese Academy of Sciences, Shanghai 200050, P. R. China

† These authors contributed equally to this work

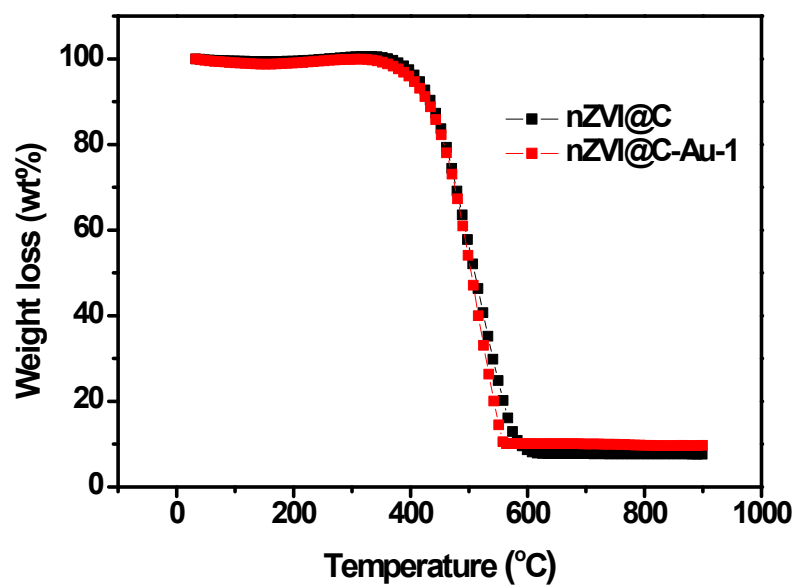


Figure S1. TG curves of the nanocomposites nZVI@C by N₂ calcination at 500 °C and then H₂ reduction at 500 °C, and nZVI@C-Au-1 that is after gold extraction at 1 mg/L on the nZVI@C.

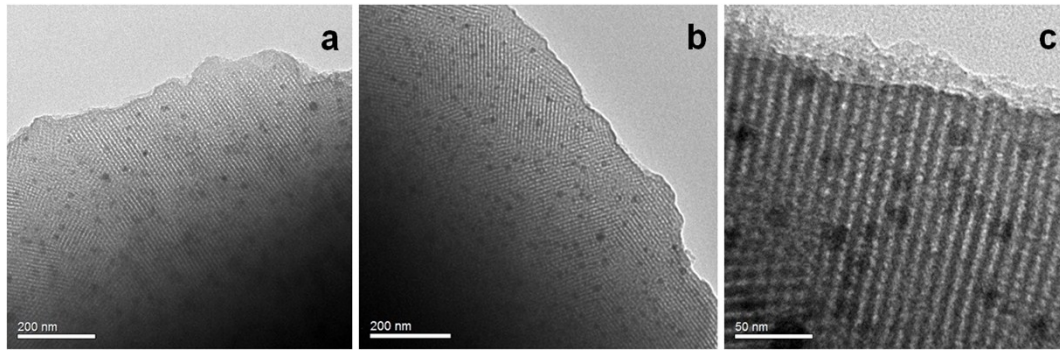


Figure S2. a) TEM images of the nanocomposites nZVI@C-300, b) 400 and c) 500 by N₂ calcination at 500 °C and then H₂ reduction at 300, 400 and 500°C, respectively.

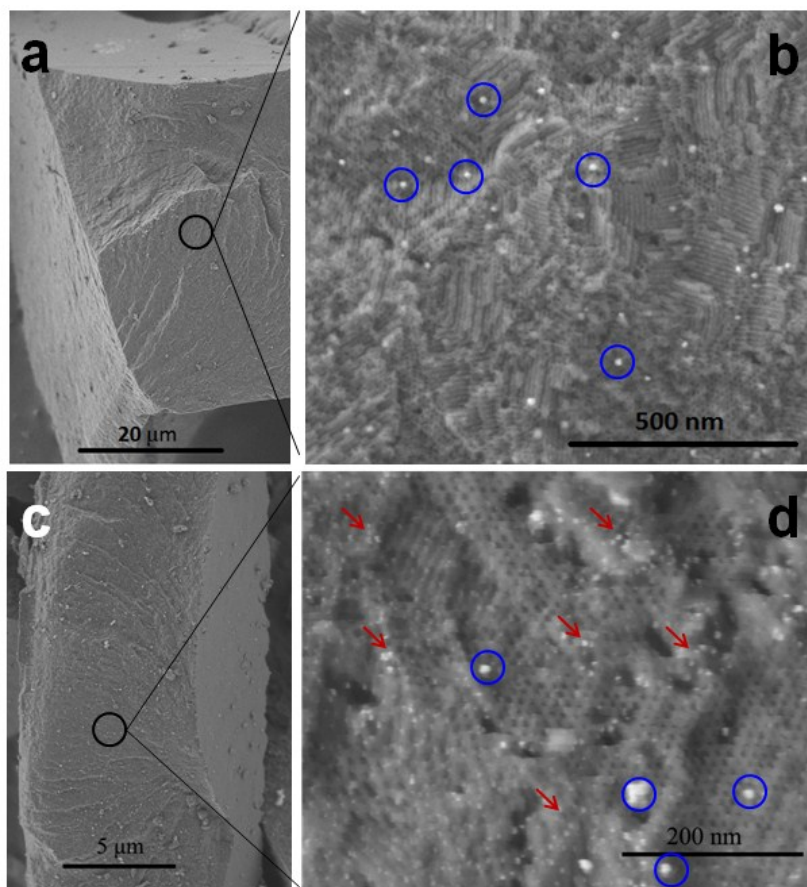


Figure S3. a, b) SEM images of the mesoporous nZVI@C-500 nanocomposite by N₂ calcination at 500 °C and then H₂ reduction at 500 °C, and c, d) the nZVI@C-Au-1 nanocomposite recovered from 1 mg/L of gold solution.

No aggregated nZVI or gold with large particle size out of the mesoporous carbon matrix can be observed over large domains from the SEM images of the nZVI@C-500 nanocomposites and nZVI@C-Au-1 nanocomposites recovered from 1 mg/L of gold initial concentration (a, c). By amplified SEM image, a very small number of iron nanoparticles with diameter ~15 nm dispersed and adhered on the surface of the mesoporous carbon matrix, which are marked by blue circle (b). After the reaction with gold solution, gold nanoparticles (~ 5 nm) are generated on the surface of the mesoporous carbon and nZVI nanoparticles, which are distinguished by red arrows (d).

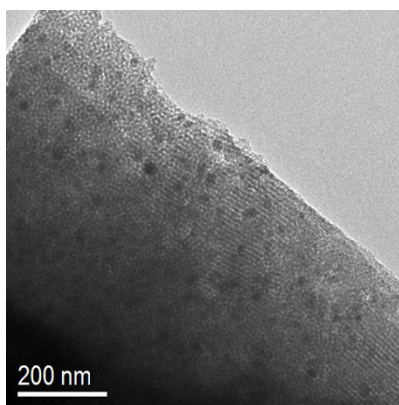


Figure S4. TEM image of the nanocomposite nZVI@C directly reduced by H₂ atmosphere at 500 °C for 3 h without N₂ treatment.

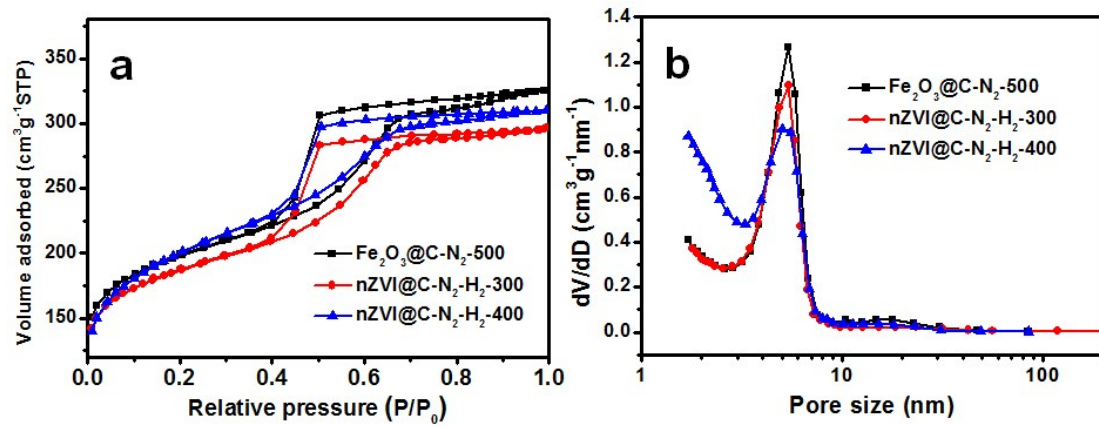


Figure S5. a) N₂ adsorption-desorption isotherms and b) the corresponding pore size distributions of the nanocomposites iron oxide@C by N₂ calcination at 500 °C and nZVI@C-300, 400 by N₂ calcination at 500 °C and then H₂ reduction at 300 and 400 °C.

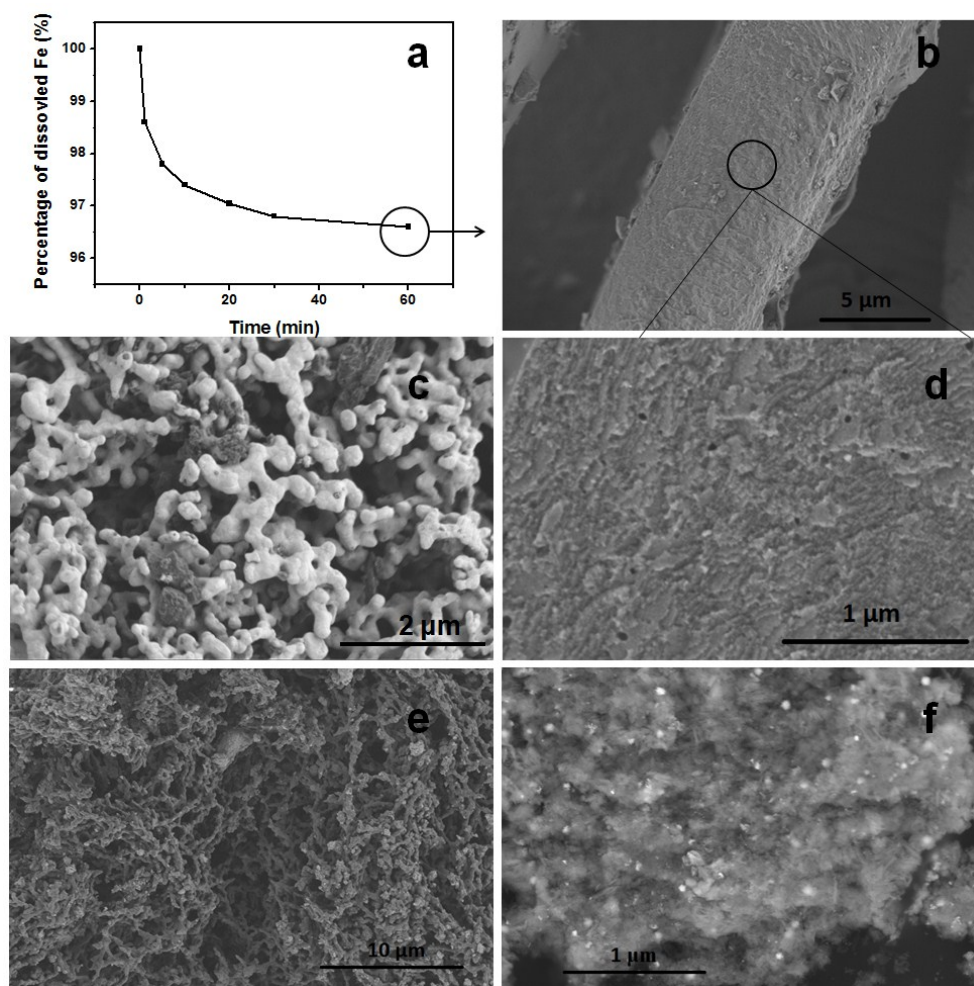


Figure S6. a) Percentage of dissolved iron in solution *versus* time at initial pH 5.0. b) SEM image and d) amplifying image of nZVI@C after leaching for 1 h at initial pH 5.0 absence of gold ions. c) SEM image of the nZVI@C-Au-30 nanocomposite recovered from 30 mg/L of gold solution. SEM image of nZVI nanoparticles without supports d) before and e) after gold extraction at initial concentration of 1 mg/L.

Zero-valent iron leaching experiment under control conditions (no gold present) at initial pH 5.0, after 1 h reaction, about ~ 2.5% of nZVI are dissolved. From the SEM observation (b, d), no obvious iron nanoparticles can be found on the surface of the mesoporous carbon in large domains, indicating main dissolution process of iron may occur on the surface.

High concentration with initial gold solutions of 30 mg/L is adopted for comparison. SEM image (c) shows that the gold particles grow up to micrometer-scale but not ultra-tiny nanometer-scale. It suggests that the process is Ostwald ripening one. When

the concentration of solution is low (< 1 mg/L), the gold approaches to nucleate explosively and generate very small nanoparticles; while the concentration is too high (30 mg/L), the small nanoparticles tend to become larger particles out of the mesopore channels according to the Ostwald ripening.

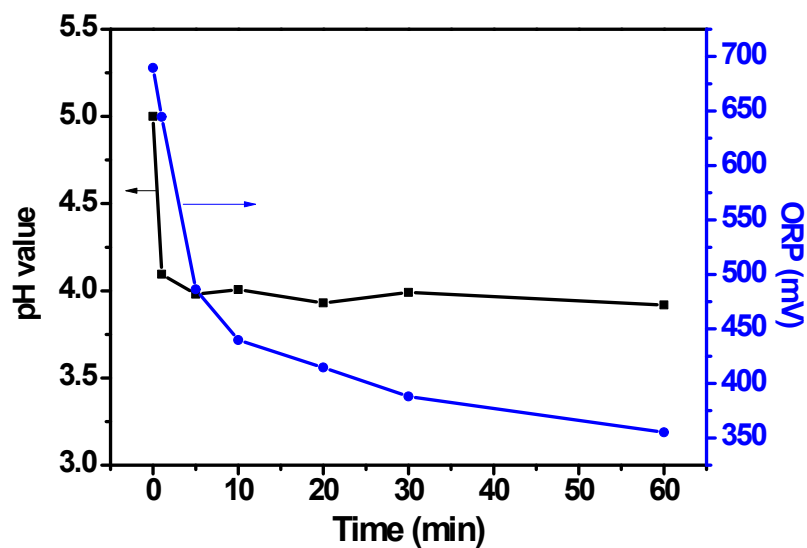


Figure S7. The pH and ORP values *versus* reaction time in aqueous solution of nZVI@C nanocomposite at initial gold concentration of 1 mg/L.

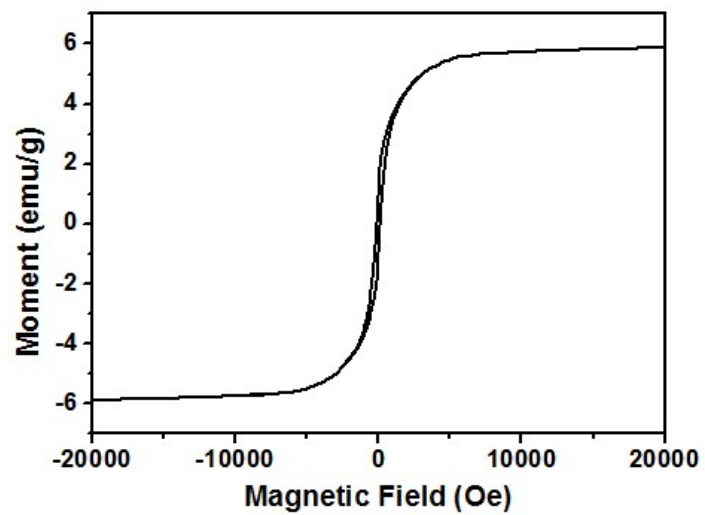


Figure S8. Magnetization curve of nZVI@C-Au-1 nanocomposite (nZVI@C recovered from 1 mg/L of gold solution).

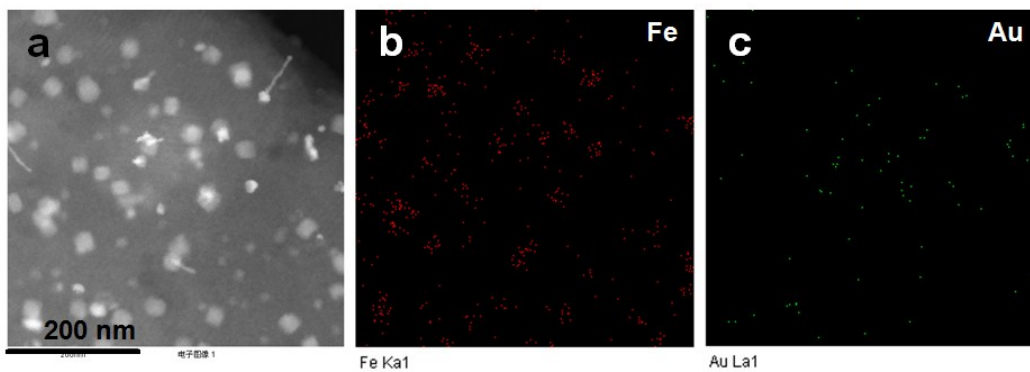


Figure S9. a) STEM image and b, c) EDS mapping of the nZVI@C-Au-1 nanocomposites recovered from 1 mg/L of gold solution.

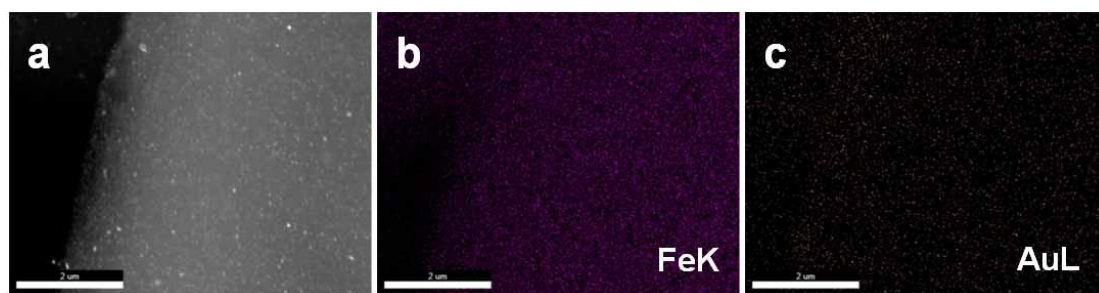


Figure S10. a) SEM image and b, c) mapping of the nZVI@C-Au-1 nanocomposites recovered from 1 mg/L of gold solution.

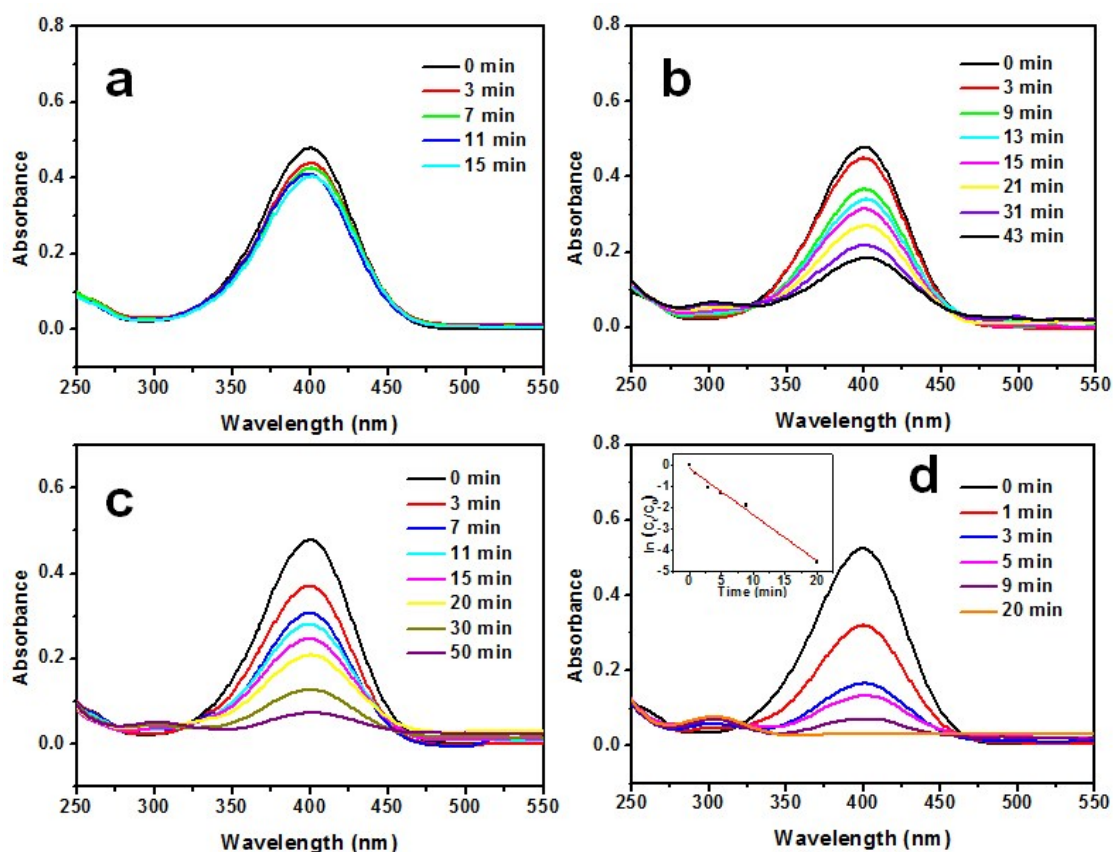


Figure S11. a) UV-vis spectra of 4-nitrophenol adsorption/reduction *versus* time in aqueous solution by mesoporous carbon, b) nZVI@C-Au-30 nanocomposite recovered from 30 mg/L of gold solution, c) nZVI@C without gold extraction, d) and nZVI@C-Au-1 nanocomposite after seven times of recycling and its corresponding relationship between $\ln(C_t/C_0)$ and reaction time (d inset).

When NaBH_4 is added, the maximum adsorption peak of aqueous 4-NP solution shifts from 317 to 400 nm due to the formation of 4-nitrophenolate. No obvious change in the absence of the catalyst indicates that the reduction reaction does not proceed.

Pure mesoporous carbon matrix was added in the same solution which the nZVI@C-Au-1 added for control experiment to study the effect of adsorption (a). The results show that the peak intensity at 400 nm decreases 15 % after 15 min, but no new one generates around 291 nm, suggesting that adsorption occurs on the surface of the carbon matrix. Furthermore, the nanocomposites nZVI@C without gold extraction

and nZVI@C-Au-30 with a large particle size of gold are adopted as catalysts for comparison. Both of the catalysts show inferior reduction performance for 4-NP (b, c). These results suggest that nZVI nanoparticles play an auxiliary role on reduction of the 4-NP, and the size of gold nanoparticles are too large to facilitate the catalysis. The high reaction activity of nZVI@C-Au-1 origins from the synergistic effect of three-component system: (i) stable, ultra-small and dispersed gold nanoparticles for highly efficient catalysis; (ii) carbon matrix providing adsorption ability to 4-NP *via* π - π stacking interactions, which offers a high concentration of 4-NP near the gold nanoparticles for a more efficient contact between them; (iii) nZVI nanoparticles play auxiliary roles on the reduction of 4-NP.

nZVI@C-Au-1 nanocomposites after seven times of recycling (d), the reaction rate decreases a little to 0.21 min^{-1} , implying that adsorption of the carbon matrix and reduction of the nZVI give a synergistic effect for adsorption and reduction at first.

Table S1 Structural and textural properties of the iron-containing mesoporous carbon prepared with various conditions.

Sample	a_0 (nm)	S_{BET} (m ² g ⁻¹)	V_t (cm ³ g ⁻¹)	D (nm)	Wall thickness (nm)
Iron oxide@C-500	11.3	690	0.54	5.2	6.1
nZVI@C-300	11.3	670	0.51	5.2	6.1
nZVI@C-400	11.2	700	0.48	5.2	6.0
nZVI@C-500	10.8	770	0.53	5.3	5.5
nZVI@C-Au-1	--	600	0.45	4.9	--

Table S2 Comparison of gold extraction.

Au concentration (mg/L)	Material	Au removal (%,30 min)	Au removal (%,final)	Time (h)	Ref.
47	Functional resin	< 10	98	24	1
25	Chitosan derivative	50	95	6	2
100	Modified polymer beads	11	90	2	3
16	Activated carbon	--	85	1	4
1	nZVI@C	> 99	> 99	0.08	Our work
0.1	nZVI@C	> 99	> 99	0.08	Our work

References

- 1 D. Jermakowicz-Bartkowiak, *React. Funct. Polym.*, 2007, **67**, 1505.
- 2 M. L. Arrascue, H. M. Garcia, O. Horna and E. Guibal, *Hydrometallurgy*, 2003, **71**, 191.
- 3 R. R. Gonte and B. K., *J. Hazard. Mater.*, 2012, **217–218**, 447.
- 4 O. N. Kononova, A. G. Kholmogorov, N. V. Danilenko, S. V. Kachin, Y. S. Kononov and Z. V. Dmitrieva, *Carbon*, 2005, **43**, 17.